



This is a repository copy of *OC-0182: A comparison of CT ventilation with 3He and 129Xe MRI for functional avoidance treatment planning.*

White Rose Research Online URL for this paper:  
<http://eprints.whiterose.ac.uk/160342/>

Version: Published Version

---

**Proceedings Paper:**

Tahir, B., Hughes, P., Robinson, S. et al. (10 more authors) (2018) OC-0182: A comparison of CT ventilation with 3He and 129Xe MRI for functional avoidance treatment planning. In: Radiotherapy and Oncology. ESTRO 37, 20-24 Apr 2018, Barcelona, Spain. Elsevier BV , S96-S97.

[https://doi.org/10.1016/s0167-8140\(18\)30492-4](https://doi.org/10.1016/s0167-8140(18)30492-4)

---

**Reuse**

This article is distributed under the terms of the Creative Commons Attribution-NonCommercial-NoDerivs (CC BY-NC-ND) licence. This licence only allows you to download this work and share it with others as long as you credit the authors, but you can't change the article in any way or use it commercially. More information and the full terms of the licence here: <https://creativecommons.org/licenses/>

**Takedown**

If you consider content in White Rose Research Online to be in breach of UK law, please notify us by emailing [eprints@whiterose.ac.uk](mailto:eprints@whiterose.ac.uk) including the URL of the record and the reason for the withdrawal request.



[eprints@whiterose.ac.uk](mailto:eprints@whiterose.ac.uk)  
<https://eprints.whiterose.ac.uk/>

Table. Performance of the reference and the MR-IBM model in training (Center A) and external validation cohort (Center B)

	Reference model		MR-IBM model	
	PG dose		PG dose	
	$Xe^{T_{baseline}}$		$Xe^{T_{baseline}}$	
	Train	Extern val.	Train	Extern val.
AUC	0.81	0.65	0.88	0.83
	(0.71-0.91)		(0.79-0.96)	
$R^2$	0.39	0.07	0.51	0.36
$AUC_{bootstrapped}$	0.78	-	0.83	-
$R^2_{bootstrapped}$	0.32	-	0.39	-

MR-IBM: Magnetic Resonance Image Biomarker;  $Xe^{T_{baseline}}$ : xerostomia at baseline; PG dose: mean dose to parotid glands; P90: 90th percentile of MR intensities; AUC: Area Under the Curve; Train: model development Center A dataset; External val.: externally validated in Center B dataset

#### OC-0181 Two common methods of defining functional lung, using SPECT and 4D-CT, do not obtain the same voxels

T. Nyeng<sup>1</sup>, L. Hoffmann<sup>1</sup>, K. Farr<sup>2</sup>, A. Khalil<sup>2</sup>, C. Grau<sup>2</sup>, D. Møller<sup>1</sup>

<sup>1</sup>Aarhus University Hospital, Department of Oncology-Medical Physics, Aarhus, Denmark

<sup>2</sup>Aarhus University Hospital, Department of Oncology, Aarhus, Denmark

##### Purpose or Objective

High rates of local recurrence and tissue toxicity often impedes radiotherapy (RT) of advanced lung cancer (LC). Many patients develop radiation-induced pneumonitis (RP), and the incidence is commonly associated with dose and volume parameters, as e.g. the mean lung dose. However, recent studies have shown that dose to the highly functional lung (FL) correlates better with RP rates than dose to the total lung, suggesting that RP rates can be lowered by prioritising avoidance of FL in treatment planning. Characterisation of FL in lung cancer patients is commonly obtained by use of perfusion (Q) single photon emission computed tomography (SPECT) identifying the best perfused areas of lung, or by deriving ventilation (V) information from four-dimensional (4D) computed tomography (CT) scans, identifying the best ventilated areas of lung. Both methods have been demonstrated to produce FL volumes that correlate better with RP rates than conventional anatomical lung dose-volume measures. It has not been investigated though, whether or not the methods define the same voxels of lung as highly functional.

##### Material and Methods

Perfusion and ventilation based FL volumes for 30 retrospective patients receiving RT for non-small cell lung cancer (NSCLC) were derived using a Q-SPECT and 4D-CT scan both obtained pre-treatment. The FL volume from Q-SPECT,  $V_{FL-SPECT}$ , was defined as the voxels within the total lung volume ( $V_{L_{Tot}}$ ) with values exceeding a threshold of 40% of the maximum perfusion count. The ventilation based FL volumes were obtained from the 4D-CT scans by deformable registration of the exhale to the inhale phase. The expansion was identified as values of the Jacobian determinant of the deformation vector field ( $J_{DVF}$ ) above 1. The FL volume from the 4D-CT registration was defined as the voxels with  $J_{DVF} > 15\%$  of the maximum  $J_{DVF}$ , resulting in volumes comparable in size to the Q-SPECT FL volumes. Overlap fractions, defined as  $(V_{FL-SPECT} \cap V_{FL-4Dvent}) / \text{Min}[V_{FL-SPECT}, V_{FL-4Dvent}]$ , were calculated between the two FL volumes. Example of FL segmentation in Fig1.

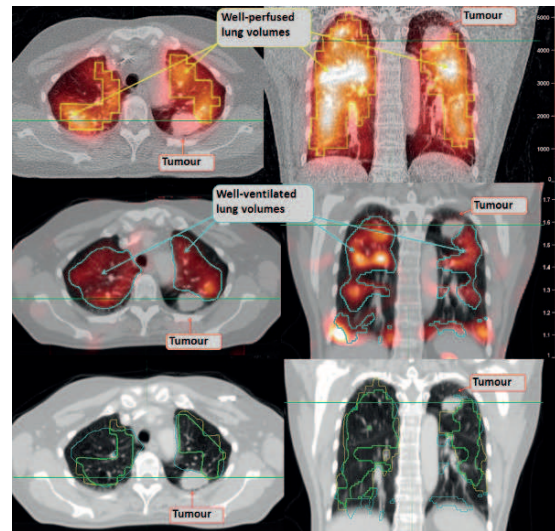


Fig1: Functional lung (FL) segmentations using two different methods for the same patient (green lines indicate corresponding imaging planes): **Top:** Q-SPECT-CT, yellow contour is the best perfused volumes of lung tissue. **Middle:** Planning (mid-ventilation) phase of 4D-CT and ventilation map, cyan contour indicates the best ventilated volume within the lung. **Bottom:** Planning (mid-ventilation) phase of 4D-CT, contours shown are Q-FL (yellow) and V-FL (cyan), and the overlap of these volumes (green).

##### Results

FL volumes of the 30 patients defined by Q-SPECT and 4D-CT ventilation maps were comparable in size, with a median[range] of  $1203\text{cm}^3$ [928-2340] and  $1181\text{cm}^3$ [782-1858], respectively. The median overlap fraction of the FL volumes was 56%[34-65]. The median overlapping volume, i.e. the volume defined as FL by both methods, was 18%[6-24] of the  $V_{L_{Tot}}$ . The union of the two types of FL volumes corresponded to a median 55%[34-63] of  $V_{L_{Tot}}$ .

##### Conclusion

The two common methods of defining FL obtain volumes that are only partly overlapping, though both have been reported to predict RP outcome. This indicates that dose sparing of both well ventilated and well perfused parts of the lungs impact the RP risk. This information has not previously been combined. Before incorporating FL avoidance into treatment planning for NSCLC, a thorough investigation of the combination of Q-SPECT and 4D-CT ventilation map FL volumes most predictive of RP is required.

#### OC-0182 A comparison of CT ventilation with <sup>3</sup>He and <sup>129</sup>Xe MRI for functional avoidance treatment planning

B. Tahir<sup>1,2</sup>, P. Hughes<sup>2</sup>, S. Robinson<sup>1,2</sup>, H. Marshall<sup>2</sup>, N. Stewart<sup>2</sup>, A. Biancardi<sup>2</sup>, H.F. Chan<sup>2</sup>, G. Collier<sup>2</sup>, K. Hart<sup>1</sup>, J. Swinscoe<sup>1</sup>, M. Hatton<sup>1</sup>, J. Wild<sup>2</sup>, R. Ireland<sup>1,2</sup>

<sup>1</sup>University of Sheffield, Academic Unit of Clinical Oncology, Sheffield, United Kingdom

<sup>2</sup>University of Sheffield, Academic Radiology, Sheffield, United Kingdom

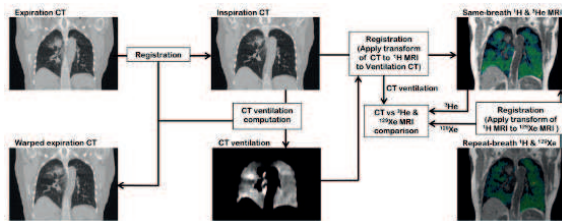
##### Purpose or Objective

CT-based surrogates of regional ventilation ('CT ventilation') which are derived from deformably registered non-contrast pulmonary CT images acquired at different inflation levels have been proposed for functional lung avoidance radiotherapy planning and are currently the subject of three US clinical trials (NCT02528942, NCT02308709, NCT02843568). However, their physiological accuracy has yet to be fully validated against a direct ventilation imaging modality. Here, we develop an image acquisition and analysis strategy to facilitate direct spatial correlation of CT ventilation with both hyperpolarised <sup>3</sup>He and <sup>129</sup>Xe MRI and apply it to a cohort of lung cancer radiotherapy patients.

##### Material and Methods

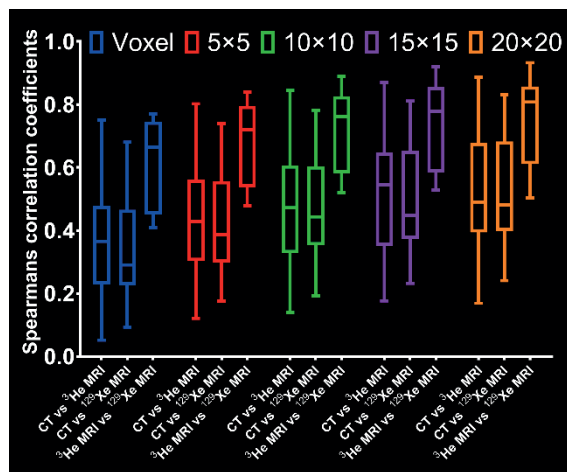
11 lung cancer patients undergoing radiotherapy underwent expiratory and inspiratory breath-hold CT.

$^{129}\text{Xe}$  and  $^1\text{H}$  MRI were also acquired at the same inflation state as inspiratory CT. This was followed immediately by acquisition of  $^3\text{He}$  and  $^1\text{H}$  MRI in the same breath and at the same inflation state as inspiratory CT. Expiration CT was deformably registered to inspiration CT for calculation of CT ventilation from voxel-wise differences in Hounsfield units. Inspiration CT and the  $^{129}\text{Xe}$  MRI's corresponding anatomical  $^1\text{H}$  MRI were registered to  $^3\text{He}$  MRI via its same-breath anatomical  $^1\text{H}$  MRI. All registrations were performed using the ANTs registration suite. The workflow is shown in Figure 1. Spatial correlation was assessed by computing the voxel-wise Spearman correlation coefficients between each CT ventilation image and its corresponding  $^3\text{He}/^{129}\text{Xe}$  MR image and for the mean values in corresponding regions of interest (ROIs), ranging from finer to coarser in-plane dimensions of 5 by 5, 10 by 10, 15 by 15 and 20 by 20, located within the lungs as defined by the same-breath  $^1\text{H}$  MRI lung mask. As a secondary analysis in order to establish scan-to-scan similarity between  $^3\text{He}$  and  $^{129}\text{Xe}$  MRI, Spearman coefficients were assessed at the voxel-level and for the same ROIs detailed above.



## Results

The Spearman's coefficients at the voxel level and for a range of corresponding ROIs of CT ventilation,  $^3\text{He}$  and  $^{129}\text{Xe}$  MRI for all patients are shown graphically as a box plot in Figure 2.



## Conclusion

This work demonstrates an image acquisition protocol and analysis strategy to facilitate a direct spatial correlation of CT-based surrogates of ventilation against hyperpolarised  $^3\text{He}$  and  $^{129}\text{Xe}$  gas MRI. This methodology was tested in a cohort of lung cancer patients. Moderate correlations of CT at the voxel level against both hyperpolarised gases, increasing for more coarser regional analysis, were observed. Discrepancies could be attributable to a number of factors including non-ventilatory effects due to blood volume changes between inflation states which are not accounted for in the CT ventilation models, the inherent noise in CT intensity, and registration errors at the voxel-level. In all cases, the correlation was significantly less than for  $^3\text{He}$  vs  $^{129}\text{Xe}$  MRI.

## Proffered Papers: PH 4: Inter- and intra- fractional motion

### OC-0183 A case-control study of the relations between planned vs actually delivered rectal dose surface maps

O. Casares Magaz<sup>1</sup>, S. Bülow<sup>1</sup>, N. Pettersson<sup>2</sup>, V. Moiseenko<sup>3</sup>, M. Thor<sup>4</sup>, J. Einck<sup>3</sup>, A. Hopper<sup>3</sup>, R. Knopp<sup>3</sup>, L. Muren<sup>1</sup>

<sup>1</sup>Aarhus University Hospital, Medical Physics - Oncology, Aarhus, Denmark

<sup>2</sup>Sahlgrenska University Hospital, Medical Physics, Gothenburg, Sweden

<sup>3</sup>University of California San Diego, Radiation Medicine and Applied Sciences, San Diego, USA

<sup>4</sup>Memorial Sloan Kettering Cancer Center, Medical Physics, New York, USA

### Purpose or Objective

Modern radiotherapy (RT) protocols for prostate cancer often include the use of narrow margins combined with careful image-based control of the rectum/bladder filling status during therapy. These techniques have allowed safe dose escalation to the prostate, however, the risk of late gastrointestinal (GI) toxicity associated with rectal irradiation is still a major dose limiting factor. The associations between GI toxicity and spatial dose distributions within the rectum/rectal wall are not fully understood, possibly due to differences between planned and actually delivered dose distributions. By using parameterized rectal 2D dose surface maps (DSM) in the setting of high-precision RT for prostate cancer, the aim of this study was to evaluate differences in spatial dose distributions between patients with and without late GI toxicity.

### Material and Methods

A case-control study was performed within a cohort of 449 prostate cancer patients treated to a prescription dose of 77.4-81.0 Gy using daily cone beam CT (CBCT)-based image-guided VMAT/IMRT. Planning CT and RT delivery adhered to a full bladder/empty rectum protocol, where daily CBCTs were used for patient realignment and to assess bladder and rectum filling status. Each of the six cases presenting with late RTOG GI  $\geq$  Grade 2 toxicity was matched with three controls based on: pretreatment GI symptoms, age  $\pm$  5y, risk group (low, intermediate, high), RT technique (VMAT/IMRT) and use of neoadjuvant androgen deprivation therapy. Fourteen CBCTs per patient were rigidly registered to the planning CT using the recorded treatment shifts, and the rectum was manually contoured on each CBCT. Contours were reviewed and approved by the responsible radiation oncologist. For the planning CT and for each CBCT, the rectum was digitally unfolded using a contour-based method to create a parameterized DSM. Dose distributions of DSMs were compared using permutation t-tests between the planned and the delivered maps (i.e. the weighted average of the CBCT-based maps), and between cases and controls.

### Results

Similar rectum volumes and cross sectional areas were observed in the planning CT and in the CBCTs. No significant differences were observed in population-average DSM between planned and delivered (permutation t-test, adjusted p-value = 0.82, Fig. 1). The cases tended to have higher doses delivered at the inferior part of the rectum, compared to controls (permutation t-test, adjusted p-value = 0.15, Fig. 2). In contrast, higher doses were observed at the central part of the DSM for controls compared to cases (permutation t-test, adjusted p-value = 0.02).